Available online at www.sciencedirect.com
ScienceDirect
Biochimica et Biophysica Acta 1768 (2007) 705–714
Biochimica et Biophysica Acta
BBA
www.elsevier.com/locate/bbamem

# Association of vasoactive intestinal peptide with polymer-grafted liposomes: Structural aspects for pulmonary delivery

Brigitte Stark [a], Paul Debbage [b], Fritz Andreae [c], Wilhelm Mosgoeller [d], Ruth Prassl [a,*]

[a] *Institute of Biophysics and Nanosystems Research, Austrian Academy of Sciences, Schmiedlstr.6, A-8042 Graz, Austria*
[b] *Department of Anatomy, Histology and Embryology, Medical University of Innsbruck, Innsbruck, Austria*
[c] *piCHEM Research and Development, Graz, Austria*
[d] *Institute of Cancer Research, Medical University of Vienna, Vienna, Austria*

Received 20 September 2006; received in revised form 25 October 2006; accepted 24 November 2006
Available online 15 December 2006

**Abstract**

A polymer-grafted liposomal formulation that has the potential to be developed for aerosolic pulmonary delivery of vasoactive intestinal peptide (VIP), a potent vasodilatory neuropeptide, is described. As VIP is prone to rapid proteolytic degradation in the microenvironment of the lung a proper delivery system is required to increase the half-life and bioavailability of the peptide. Here we investigate structural parameters of unilamellar liposomes composed of palmitoyl-oleoyl-phosphatidylcholine, lyso-stearyl-phosphatidylglycerol and distearyl-phosphatidyl-ethanolamine covalently linked to polyethylene glycol 2000, and report on VIP–lipid interaction mechanisms. We found that the cationic VIP is efficiently entrapped by the negatively charged spherical liposomes and becomes converted to an amphipathic α-helix. By fluorescence spectroscopy using single Trp-modified VIP we could show that VIP is closely associated to the membrane. Our data suggest that the N-terminal random-coiled domain is embedded in the interfacial headgroup region of the phospholipid bilayer. By doing so, neither the bilayer thickness of the lipid membrane nor the mobility of the phospholipid acyl chains are affected as shown by small angle X-ray scattering and electron spin resonance spectroscopy. Finally, in an *ex vivo* lung arterial model system we found that liposomal-associated VIP is recognized by its receptors to induce vasodilatory effects with comparable high relaxation efficiency as free VIP but with a significantly retarded dilatation kinetics. In conclusion, we have designed and characterized a liposomal formulation that is qualified to entrap biologically active VIP and displays structural features to be considered for delivery of VIP to the lung.


*Keywords:* Polyethlene glycolated liposome; Sterically stabilized liposome; Nanostructure; Amphipathic peptide; Peptide–lipid interaction

## 1. Introduction

Vasoactive intestinal peptide (VIP) is a cationic mammalian neuropeptide that exerts multiple biological functions including systemic and pulmonary vasodilation, bronchodilatation, anti-inflammatory and immunomodulatory effects [1–3]. The function of VIP is mediated by a specific receptor class, VPAC1 and VPAC2, and both receptors being highly expressed in the bronchial tree and in the pulmonary vasculature [4,5]. This contributes to the fact that VIP can be considered as a therapeutic agent for severe lung diseases such as primary pulmonary hypertension (PPH) or chronic obstructive pulmonary disease (COPD). In PPH the blood pressure in the pulmonary artery rises far above normal levels. Untreated, the median period of survival for PPH is 3 years following diagnosis [6]. Common to all PPH patients is the lack of VIP in serum, together with an upregulation of VIP receptors in the lung [6]. It has been shown that aerosolic applications of VIP can halt the progression of the disease and may relieve the symptoms. However, the clinical application of VIP is severely limited by the fact that VIP is prone to rapid proteolytic digestion and inactivation by neutral endopeptidases, reducing the efficiency and bioavailability of the peptide [7–9]. For these reasons it is an ongoing need to establish a proper delivery system for aerosolic application of VIP.

The structural versatility of lipid species and the use of lipid mixtures and co-additives make liposomes excellent carriers for

* Corresponding author. Tel: +43 316 4120 305; fax: +43 316 4120 390.
*E-mail address:* ruth.prassl@oeaw.ac.at (R. Prassl).

0005-2736/$ - see front matter © 2006 Elsevier B.V. All rights reserved.
doi:10.1016/j.bbamem.2006.11.017

therapeutic drugs to be used for different medical applications [10–13]. In particular, polymer surface coated liposomes, known as sterically stabilized liposomes have been shown to exhibit a longer life-time in the circulation [14–20].

To date most liposomal formulations have been designed for intravenous application and delivery of small molecules. Nonetheless, the way should also be opened for the delivery of peptides by alternate administration routes such as pulmonary delivery by inhalation.

However, to act as potent carrier for peptides to the lung, the delivery system has to meet certain criteria. First, the liposomal formulation has to be stable and of optimal size to reach the lower bronchioles [21]. Second, the liposomes have to accommodate sufficient amounts of peptide and shield their payload from enzymatic degradation in the pulmonary microenvironment.

In this study we have used a ternary lipid mixture that self-assembles to form sterically stabilized unilamellar liposomes. The liposomes are composed of phosphatidylcholine as lipid matrix combined with polyethyleneglycol-grafted phosphatidylethanolamine and lyso-phosphatidylglycerol. Since this formulation has not been described so far we aimed to characterize it and to address the question of its suitability as peptide carrier. Accordingly, it was important to examine the impact of peptide loading both on particle stability and integrity. In particular, the structural features of the self-associated peptide in the presence of lipids and the interaction mechanisms with the lipid bilayer were investigated in detail. These structural data might also be important in respect to receptor binding and cellular processes [5,22]. Finally, the biological response of living lung arteries to liposomal-associated VIP was tested in terms of vasorelaxation activities.

## 2. Materials and methods

Palmitoyl-oleoyl-phosphatidylcholine (POPC), lyso-stearyl-phosphatidylglycerol (lyso-PG) and polyethyleneglycol conjugated distearyl-phosphatidylethanolamine (DSPE-PEG2000) were purchased from Avanti Polar Lipids (Alabaster, AL).

Acetylcholine chloride, L-phenylephrine hydrochloride and all other chemicals were purchased from Sigma-Aldrich, Vienna, Austria.

VIP (amino-acid sequence HSDAVFTDNYTRLRKQMAVKKYLNSILN-NH2), VIP C-terminally labeled with the fluorescent marker Cy3 (VIP(Cy3)) and three different tryptophan (Trp) modified VIP species, namely N-terminally modified VIP ($Trp^1$VIP), C-terminally modified VIP ($Trp^{29}$VIP) and Trp inserted at position 16 of the amino acid sequence of VIP ($Trp^{16}$VIP) were synthesized by piCHEM (Graz, Austria) using FMOC-solid-phase peptide synthesis methodology (FMOC-SPPS). The peptides were purified by RP-HPLC.

### 2.1. Nanoparticle preparation

Stock solutions of DSPE-PEG2000, lyso-PG and POPC were prepared in chloroform and chloroform:methanol 9:1 and 2:1 (v/v), respectively. Aliquot amounts of lipid stock solutions were mixed to yield a molar ratio of DSPE-PEG-2000: lyso-PG: POPC of 5: 38: 57 mol% with a total lipid content of 30 mg. The organic solvents were evaporated under a stream of nitrogen. Residual traces of solvent were removed in high vacuum overnight. The dry lipid film was suspended in 1 mL buffer consisting of 10 mM Tris–HCl, pH: 7.4 (Tris-buffer) and hydrated at 40 °C for 60 min with repeated vortexing. For peptide loading hydration was performed with 1 mL Tris-buffer containing 0.5 mg VIP (corresponding to a molar phospholipid to VIP ratio of 250:1). Peptide loading was quantified using fluorescent labeled peptide (VIP(Cy3)) and separation by gel filtration chromatography using a Sephadex G 75 column (Amersham Biosciences, Uppsala, Sweden). VIP(Cy3) eluted as a single band together with the liposomes. In comparison, free VIP(Cy3) used as control, did not show a single band, but smeared along the column.

When appropriate, lipid suspensions were extruded 21 times through polycarbonate filters (Millipore, Vienna Austria) with 100 nm pore size using a LiposoFast pneumatic extruder (Avestin, Inc. Ottawa, ON). If not stated otherwise, non-extruded liposomes were used for the experiments.

Phospholipid concentration was determined by a modified Bartlett inorganic phosphate assay [23].

### 2.2. Photon correlation spectroscopy (PCS)

The particle size of the liposomes was determined by photon correlation spectroscopy (PCS) with a Zetasizer 3000 HSA (Malvern Instruments, Herrenberg, Germany). The instrument was equipped with a 10 mW helium-neon laser operating at 632.8 nm. The scattered light was detected at an angle of 90° by a photon counting avalanche photodiode detector coupled to a correlator. Particle size is derived by an auto-correlation function. The results are expressed as Z-average, which is the harmonic-intensity averaged particle diameter. The width of the size distribution is given by the polydispersity index (PDI).

Empty and VIP-loaded liposomes before and after extrusion were diluted to a concentration of 0.03 mg/mL with Tris-buffer, which was previously filtered through a disposable 0.02 μm membrane filter unit (Anotop 25, Whatman International Ltd., Maidstone, UK). The measurements were performed at room temperature.

### 2.3. Transmission electron microscopy (TEM)

For electron microscopy the liposomes were fixed with 1% aqueous $OsO_4$ over night at 4 °C. A fine, cloudy precipitate formed and the clear supernatant was carefully removed. Absolute (100%) ethanol was added and after 1–2 h the precipitate condensed to form a loose pellet. The ethanol was replaced by propylene oxide as intermedium, and the pellet passed through increasing concentrations of epon in propylene oxide. The pellet was finally polymerized by incubation with epon at 60 °C for 24 h. Ultrathin sections of about 90 nm thickness were cut from the epon-embedded nanoparticle block, and double-stained with uranyl acetate and lead citrate. The sections were viewed in a Zeiss EM 10 electron microscope, images being recorded on Kodak Electron Microscope Film 4489.

### 2.4. Small angle X-ray scattering (SAXS)

Small angle X-ray scattering (SAXS) measurements were performed with an integrated SWAXS camera system (HECUS X-ray Systems, Graz, Austria) equipped with a semitransparent Ni-filtered beam-stop, a position-sensitive detector and a data collection unit. The camera was attached to a conventional Cu-anode generator (Seifert-GE ID 3003, Ahrensburg, Germany) operated at 2 kW. SAXS patterns were recorded in a $q$-range between 0.088 $nm^{-1}$ and 3.0 $nm^{-1}$, where $q=(4\pi \sin \theta)/\lambda$ is the scattering vector, $2\theta$ the scattering angle and $\lambda=0.154$ nm the wavelength of the X-ray beam. The data were buffer background corrected, normalized to intensity and corrected for slit collimation geometry. Indirect Fourier Transform of the data was performed with the program GIFT [24]. The cross-sectional structure of the bilayer was analyzed by deconvolution of the cross-section correlation function $p_t(r)$. Information about the axial thickness of the phospholipid bilayer was derived from the maximum of the $p_t(r)$ function.

SAXS measurements were performed at 20 °C with an exposure time of 1 h on empty and VIP (0.15 mM) loaded liposomes before and after extrusion at a lipid concentration of 38.5 mM.

### 2.5. Circular dichroism and secondary structure prediction

Circular dichroism (CD) spectra were recorded on a JASCO J-715 spectropolarimeter (Jasco Inc., MD, USA) in the far-UV range from 180 to 250 nm using a quartz cuvette with 2 mm cell length. A bandwidth of 1 nm with

a step resolution of 0.2 nm and a scan speed of 100 nm/min were chosen for acquisition of spectra. The average of five accumulations was taken for data evaluation. The recorded spectra for free VIP and liposomal-associated VIP (0.15 mM) were background corrected for Tris-buffer and empty liposomes, respectively. Data are expressed as the mean molar ellipticity [$\theta$] (deg cm$^2$ dmol$^{-1}$) at a given wavelength defined as:

$$[\Theta] = \frac{\Theta_{obs}}{10 \cdot c \cdot l} \quad (1)$$

where $\Theta_{obs}$ is the measured ellipticity in degrees, $c$ is the peptide residue concentration in mol/L, and $l$ is the length of the light path in cm.

The ellipticity data were analyzed for secondary structure with the use of the Web service "DichroWeb" applying the analysis algorithm CDSSTR [25,26].

The amino acid sequence of VIP was subjected to an automated secondary structure prediction service, namely PSIPRED [27,28] that is based on position-sensitive scoring matrices.

### 2.6. Fluorescence spectroscopy

Fluorescence measurements were performed on a SPEX FLUOROMAX-3 fluorescence spectrophotometer (Jobin Yvon Horiba, Longjumeau Cedex, France) using a 10 mm × 10 mm fluorescence quartz cuvette.

As Trp-modified VIP also contains tyrosine and phenylalanine residues, the excitation wavelength has to be chosen carefully to avoid the excitation of these other two aromatic amino acids. On this account tryptophan was selectively excited at 292 nm with a band width of 5 nm and an integration time of 0.1 s. The emission wavelengths were assessed between 320 and 380 nm.

Experiments were performed at room temperature with 10 μM free Trp-VIP in Tris-buffer or in a solution of PEG2000, respectively. Liposomal-associated Trp$^1$VIP, Trp$^{16}$VIP and Trp$^{29}$VIP were measured in Tris-buffer. The background intensities of Tris-buffer and empty liposomes, respectively, were subtracted before determination of emission maxima and fluorescence intensities.

#### 2.6.1. Acrylamide quenching of Trp fluorescence

Aliquots of a 3 M acrylamide stock solution were added to 10 μM free Trp-VIP in Tris-buffer or PEG2000 solution or to liposomal-associated Trp$^1$VIP, Trp$^{16}$VIP and Trp$^{29}$VIP in Tris-buffer, respectively. The acrylamide concentration was varied between 0.02 and 0.15 M. The experimental conditions were as described above.

The quenching data were analyzed with the Stern–Volmer equation

$$\frac{I_0}{I} = K_a * [Q] + 1 \quad (2)$$

where $I_0$ is the fluorescence intensity at zero quencher concentration, $I$ is the intensity at a given quencher concentration $Q$ and $K_a$ is the Stern–Volmer quenching constant of the accessible fraction.

The measured fluorescence intensities were corrected for the volume increase and the inner filter effect on the excitation beam caused by acrylamide.

The inner filter effect was corrected using the formula

$$I_{corr} = I_{abs} * anti\log\left[\frac{(A_{ex} + A_{em})}{2}\right] \quad (3)$$

where $I_{corr}$ is the corrected fluorescence intensity and $I_{abs}$ the measured one. $A_{ex}$ and $A_{em}$ are the absorption values for acrylamide at different concentrations at the excitation and emission wavelengths, respectively.

For the calculation of the Stern–Volmer quenching constants the intensity values were taken at the wavelength of the emission maximum, which was different for free and liposomal-associated VIP.

### 2.7. Electron spin resonance spectroscopy (ESR)

Liposomes were prepared as described above, but additionally contained 5-doxylstearic acid (5-DSA), a spin labeled fatty acid that probes the acyl chain region of the liposomes near the phospholipid headgoup. The molar ratio of spin label to total phospholipid was 1:60. The ESR measurements were performed with empty, Trp–VIP- and VIP-loaded liposomes.

The spectra were recorded at room temperature on an X-band ECS 106 spectrometer (Bruker, Rheinstetten, Germany) with a modulation amplitude of 1.2 G and a sweep width of the static field of 100 G.

Changes in the motional dynamics and relative orientation of the spin-probe were examined by evaluation of the outer and inner hyperfine splittings $2A_{||}$ and $2A_{\perp}$ and calculation of the corresponding order parameters $S$ (Eq. (4) and (5))

$$S = \frac{f_a(A_P - A_\perp)}{A_z - 0,5(A_x + A_z)} \quad (4)$$

where $f_a$ is the polarity correction factor derived for ESR crystal data for $A_x$, $A_y$ and $A_z$

$$f_a = \frac{A_x + A_y + A_z}{A_P + 2A_\perp} \quad (5)$$

### 2.8. Ex vivo lung arterial model system

Adult male Sprague–Dawley rats (Abteilung für Labortierkunde und Labortiergenetik, Medical University of Vienna, Himberg, Austria) weighing 250–280 g were used for the extraction/preparation of pulmonary arteries. All procedures were performed according to current national legislation. The animals were anaesthetized, lungs were excised en bloc and pinned on wax in a petri dish containing cold Krebs–Henseleit buffer (KH-buffer) in an orientation that facilitated identification of the pulmonary arteries (originating from the right ventricle). The pulmonary arterial tree was rapidly dissected from the lung parenchyma. The common pulmonary artery and the left and right extrapulmonary artery segments were opened longitudinally and divided into two pulmonary artery preparations. The preparations were cut as zigzag segments (to achieve strips of approximately 1.3 to 1.5 cm length) and mounted in thermostatically controlled (37 °C) organ baths, which contained 9 ml of KH-buffer (pH = 7.4) gassed with 95% $O_2$ and 5% $CO_2$. The arterial strips were equilibrated for 2–3 h in the organ baths. The KH-buffer was renewed three times during this process. The activity of the arterial strips under investigation was recorded isotonically under a resting load of 1 g. The arterial segments were viable for at least 4–5 h under these conditions. The mechanical signals (artery extension and contraction) were processed by bridge amplifiers (Hugo Sachs Elektronik, Germany) and recorded on ink writers.

At the beginning of each experiment the arterial reactivity was examined. This was done by precontraction of the isolated pulmonary arteries with a submaximal concentration ($EC_{80}$) of the $\alpha_1$-adrenoceptor agonist L-phenylephrine hydrochloride (Phe; 0.1 μM). Thereafter, either 100 nM free VIP or equimolar amounts of liposomal-VIP were added and the relaxation efficiency and the time period to attain the maximal relaxation were recorded. For direct comparison, experimental cycles were performed by alternate use of free or liposomal-VIP intermitted by extensive washing.

At the end of each experiment acetylcholine (1 μM) was added to control the viability of the arterial strips. In case of an acetylcholine-induced relaxation of more than 60% of the Phe-induced precontraction, the arteries were classified as intact. Only these experiments were included into the study. Empty liposomes used as a control had no impact on precontraction- or relaxation- behavior of the lung arteries. The fact that the survival rate of the arteries was not affected by liposomes indicates that at the given concentration liposomes have no cytotoxic effects on lung arteries.

### 2.9. Data and statistical analysis

Data are expressed as means ± SEM. The number of independent experiments is given as *n*.

For the statistic evaluation a Student's *t*-test was used. Statistical significance was assumed at $p < 0.05$.

Data analysis of the lung arterial experiments was performed as follows. The pre-contraction by Phe was taken as 100%. The vasorelaxation induced by

acetylcholine or VIP was taken as the percentage of the 100% precontraction. These data were transferred to a data evaluation program (SigmaPlot 8.02, SPSS Inc.) for plotting. Statistical analysis was performed with a paired sample *t*-test on consecutive exposures with free- and liposomal-VIP on the very same arteries.

Statistics were performed using the program MINITAB 13.31 (MinTab Inc.).

## 3. Results

### 3.1. Liposomal size distribution

A ternary mixture of zwitterionic PC with a saturated and an unsaturated acyl chain (POPC), anionic lyso-stearylphosphatidylglycerol (lyso-PG) and distearylphosphatidyl-ethanolamine with covalently linked polyethylene glycol with a molecular weight of 2000 (DSPE-PEG2000) was used for the preparation of liposomes by the thin film rehydration method. Hydration of the dry lipid film without further size extrusion yields unilamellar liposomes of two size populations. The main population comprises more than 95% of the particles with a mean hydrodynamic diameter of 180±10 nm ($n=7$). Up to 5% of the particles in the suspension are much larger in size, between 320 and 550 nm. The PDI values varied between 0.2 and 0.5. Subsequent size extrusion led to a highly homogeneous particle size distribution and a remarkable decrease in PDI values. A single population with a mean diameter of 91±3 nm ($n=14$) and PDI values between 0.1 and 0.2 was obtained.

The mean particle diameter of VIP-loaded liposomes was not significantly different (90±3 nm ; $p>0.5$ for $n=5$) and the PDI-values varied between 0.1 and 0.3.

To check particle stability the PCS measurements were repeated over a certain period of time. There was no significant change in mean diameter ($p=0.94$) and only a small broadening in size distribution, characterized by an increase of SEM and PDI values, was found. After a storage period of 12 weeks at 4 °C, the mean particle diameter was 91±8 nm ($n=3$) and the PDI values varied between 0.2 and 0.4.

### 3.2. Liposome morphology

To obtain additional information on particle morphology, transmission electron microscopy (TEM) was performed. TEM images taken from uranyl/lead contrasted ultrathin sections of extruded liposomes basically show hollow spheres with a size of approximately 80–100 nm (Fig. 1). These values correlated well with the results from PCS.

The smaller spherical particles seen in the images are sectioning artifacts produced by the thin cutting procedure, when only the cap of the particle is included within the section. Nevertheless, in all images a small proportion of wormlike, tubular particles are observed which represent a miniscule population of non-spheroidal nanoparticles.

### 3.3. Bilayer organization of liposomes

X-ray scattering experiments were performed to determine the lamellar organization of the particles. The scattering patterns of both, non-extruded and extruded liposomes, showed the same characteristics. We could see neither Bragg peaks, characteristic for multilamellar liposomes, nor any indication of the formation of a non-lamellar phase (Fig. 2A). Indeed, the scattering pattern is typical for the single uncorrelated bilayer of unilamellar vesicles. The single broad peak observed in the scattering pattern is related to the bilayer thickness. Thus, a one-dimensional thickness distance distribution function $p_t(r)$ was calculated and revealed a cross-sectional phospholipid head-group distance of ~4.2 nm (Fig. 2B). Interestingly, the $p_t(r)$ function shows a small side maximum at higher r-values. This side maximum probably arises from the PEG-chains, which protrude from the phospholipid bilayer as less densely packed hydrophilic shell [29]. At a concentration of 5 mol% DSPE-PEG2000 the PEG-lipid chains extend 4.5 to 6.5 nm from the bilayer surface, depending on the lipid matrix used [29–31] and might well contribute to the scattering pattern.

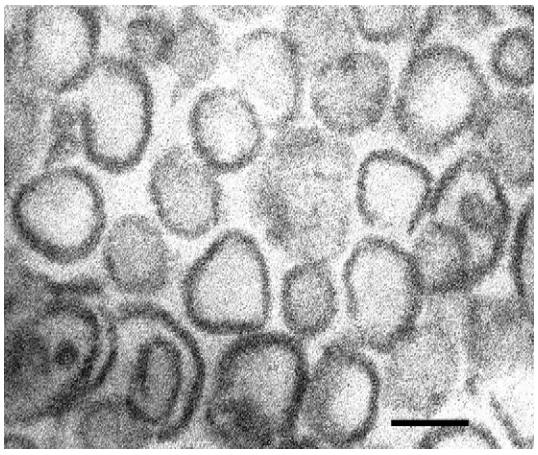

Fig. 1. Transmission electron microscopic image of extruded liposomes. The liposomes were osmium-fixed, epon-embedded and ultrathin sections, about 90 nm thick, were cut and uranyl/lead stained. Original magnification 80000×. Calibration bar: 100 nm.

Likewise, the scattering pattern and the $p_t(r)$ function of VIP-loaded liposomes showed no shift in the position of the peak maxima to higher or lower scattering angles (Fig. 2A and B). This indicates that no membrane thinning or thickening is induced by peptide interaction and that the bilayer organization is not perturbed by VIP association.

### 3.4. Secondary structure of VIP

To determine any changes in peptide conformation upon liposomal entrapment, circular dichroism spectroscopy was performed. The background corrected CD-spectra of free VIP in Tris-buffer and liposome-associated VIP are shown in Fig. 3A. In general, unfolded peptide chains show an intense minimum in the far-UV CD spectrum near 200 nm, whereas folded peptide chains are characterized by a minimum in the vicinity of 222 nm [32]. Thus, the pronounced differences in the spectral characteristics are obvious. The molar ellipticity at 222 nm was significantly increased for liposomal entrapped VIP as compared to free VIP. For free VIP about 90% random coil conformation was found whereas ~50% α-helical content was determined for liposomal VIP.

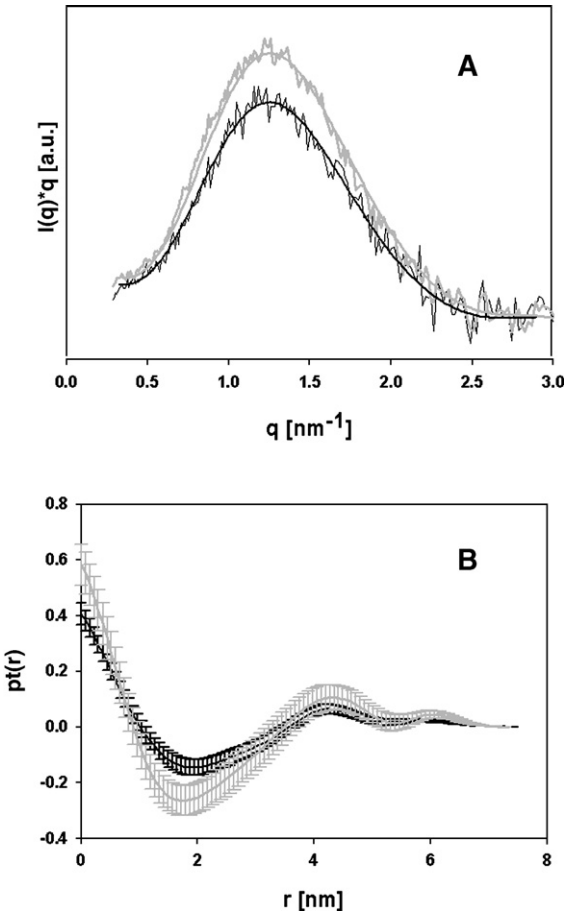


Fig. 2. SAXS pattern of empty and VIP-loaded liposomes. Panel A shows the funneled experimental scattering curves and the desmeared, approximated scattering curves of empty (grey lines) and VIP-loaded (black lines) liposomes. Panel B shows the corresponding one-dimensional thickness distribution function $p_t(r)$ showing a maximum at $r$=4.2 nm indicative for the P–P headgroup distance.

The experimental data are supported by a secondary structure prediction [33] that reveals an α-helix for the central amino acid region spanning residues Tyr$^{10}$ to Leu$^{27}$ at a high confidence level (Fig. 3B).

To assess whether VIP reveals amphipathic features we transferred the amino acid sequence, which was suggested to form an α-helix (residues 10–27), into an α-helical wheel projection (Fig. 3C). The figure shows that at least six hydrophobic amino acid residues are located on the same surface, strongly suggesting that VIP is amphiphilic in nature. Additionally, the six positively charged amino acids of VIP, which are supposed to interact with the negatively charged phospholipids of the membrane, are located on the same surface or at least at the interface to the hydrophilic surface.

### *3.5. Intrinsic Trp-fluorescence and accessibility to water-soluble quenchers*

To study the interaction of VIP with the lipid membrane, intrinsic Trp-fluorescence spectroscopy was performed. Accordingly, a single Trp-residue was attached either to the N- terminus (Trp$^{1}$VIP) or the C-terminus (Trp$^{29}$VIP) of VIP or inserted at position 16 (Trp$^{16}$VIP) of its amino acid sequence. The emission spectra of free Trp-VIP solutions showed a maximum at 355 nm, independent from the position of the Trp-residue, typical for a monomeric peptide in aqueous solution. In contrast, liposomal-entrapped Trp$^{1}$VIP showed a significant blue shift in the fluorescence emission maximum to 334 nm (Fig. 4A). This behavior is characteristic for a membrane associated peptide, in which the Trp-residue is located in a more lipophilic environment. As a control, Trp$^{1}$VIP in a solution of pure PEG2000 showed no blue-shift of the emission maximum (Fig. 4A). The spectra of liposomal- Trp$^{16}$VIP and Trp$^{29}$VIP, respectively, were blue-shifted, but not as distinct as liposomal Trp$^{1}$VIP. There was rather an intensity maximum plateau, between 335 and 345 nm,

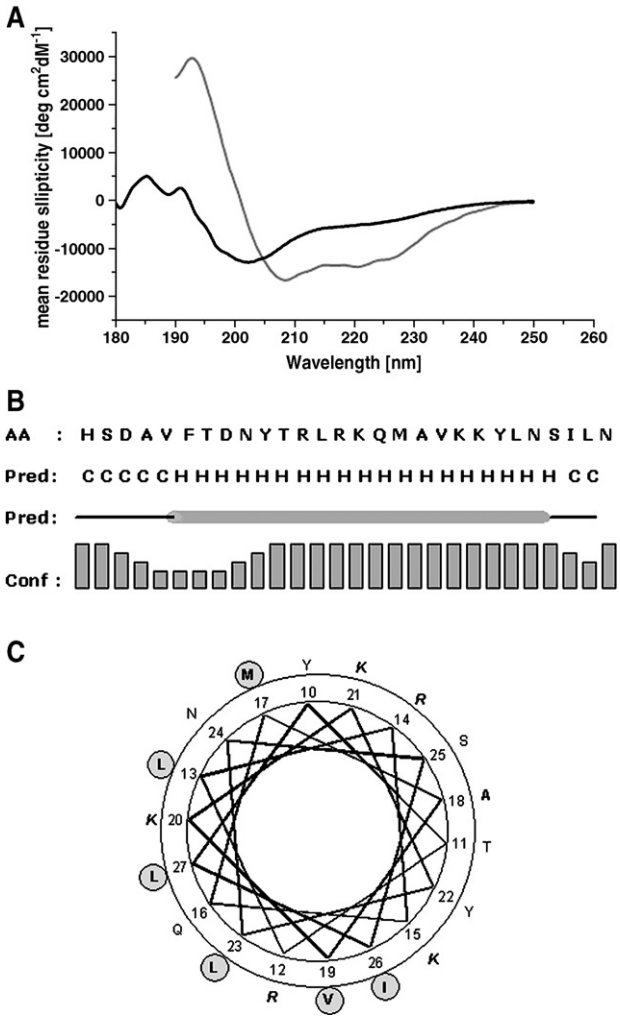


Fig. 3. Secondary structure of VIP. CD spectra of free VIP (0.15 mM) in Tris-buffer (black line) and associated with liposomes (grey line) are shown. The spectral contributions of Tris-buffer and empty liposomes, respectively, were subtracted (A). The results of a secondary structure prediction obtained by PSIPRED [33] are shown in (B). AA represents the amino acid sequence of VIP for which coil (C) and helical (H) segments are predicted. The cartoon shows the predicted helical strand as cylinder. The confidence level is shown below. A helical wheel projection was applied for the amino acid sequence with the highest confidence level for α-helical formation (C). Apolar amino acid residues are shown in bold, whereas the apolar amino acids that might form an amphipathic helix are additionally highlighted by a circle. The positively charged amino acids are shown in bold italic.

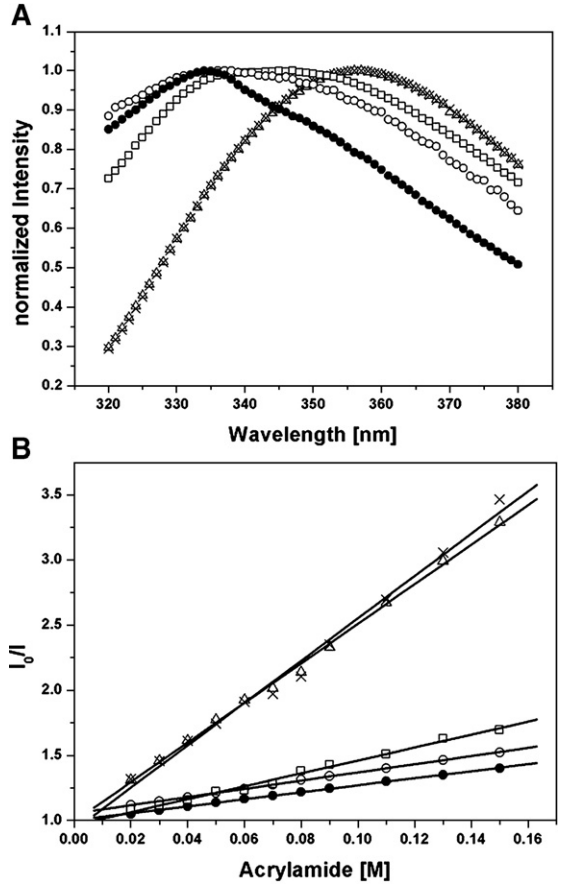


Fig. 4. Fluorescence data for free- and liposomal-VIP. Fluorescence spectra of Trp-VIP are shown as a function of normalized intensities (A). The concentration of the Trp-VIP solutions was 10 μM. Free Trp-VIP in Tris-buffer (Δ) as well as in a solution of PEG 2000 (×) showed a maximum in emission intensity at 355 nm. A pronounced shift of the emission intensity maximum to 334 nm is recorded for $Trp^1$VIP (●). For $Trp^{16}$VIP (○) and $Trp^{29}$VIP (□) broad intensity maxima are observed. (B) Stern–Volmer plot of the acrylamide quenching data of free $Trp^1$VIP in Tris-buffer (△) and in a solution of PEG2000 (×) and liposomal $Trp^1$VIP (●), $Trp^{16}$VIP (○) and $Trp^{29}$VIP (□). The acrylamide concentration was varied between 0.02 and 0.15 M. Intensity values were taken at the maximum of emission observed at 355 nm for free Trp-VIP in Tris-buffer and PEG2000 solution, respectively, and at 334 nm for all liposomal-entrapped Trp-VIP-species.

than an intensity maximum at a certain wavelength. From these data we assume that $Trp^{16}$VIP and $Trp^{29}$VIP are attached to the membrane, but do not stick into it.

To determine the accessibility of the Trp-residues, we have added the water-soluble quencher acrylamide. The Stern–Volmer quenching constants were determined according to Eq. (2) from the data shown in Fig. 4B. The $K_a$-values of the three Trp–VIP species in Tris-buffer as well as for $Trp^1$VIP in PEG2000 solution were nearly the same ($K_a$=15.2 $M^{-1}$,16.2 $M^{-1}$, 17.6 $M^{-1}$ and 16.2 $M^{-1}$ for $Trp^1$VIP, $Trp^{16}$VIP, $Trp^{29}$VIP and $Trp^1$VIP in PEG2000 solution, respectively). In contrast, a decrease in $K_a$ values was observed for all liposomal Trp–VIP species. Namely, $K_a$=2.7 $M^{-1}$, 3.1 $M^{-1}$ and 4.9 $M^{-1}$ for liposomal $Trp^1$VIP, $Trp^{16}$VIP and $Trp^{29}$VIP, respectively, being most pronounced for $Trp^1$VIP. Taken together, these data clearly reveal that liposomal VIP is shielded by the lipid bilayer and/or the PEG-surface layer and is therefore less accessible to the quencher as compared to free Trp-VIP. A pure PEG2000 solution without liposomes had no shielding effect at all.

### 3.6. Acyl chain mobility

To investigate whether VIP penetrates into the phospholipid bilayer and thereby affects the mobility of the acyl chains we incorporated a spin label in our liposomal formulation. The spin label 5-DSA probes the acyl chain region close to the phospholipid headgroups.

By examination of the spectra, values of the inner and outer hyperfine splittings were determined and order parameters $S$=0.577±0.002, 0.578±0.001 and 0.577±0.002 ($n$=3) for empty, Trp-VIP- and VIP-loaded liposomes, respectively, were calculated. The fact that the order parameters are virtually identical indicates that the acyl chain mobility is not influenced by peptide loading.

### 3.7. Vasorelaxation efficiency and kinetics

Vasorelaxation efficiency expressed as percent of maximal relaxation (precontraction value taken as 100%) and relaxation

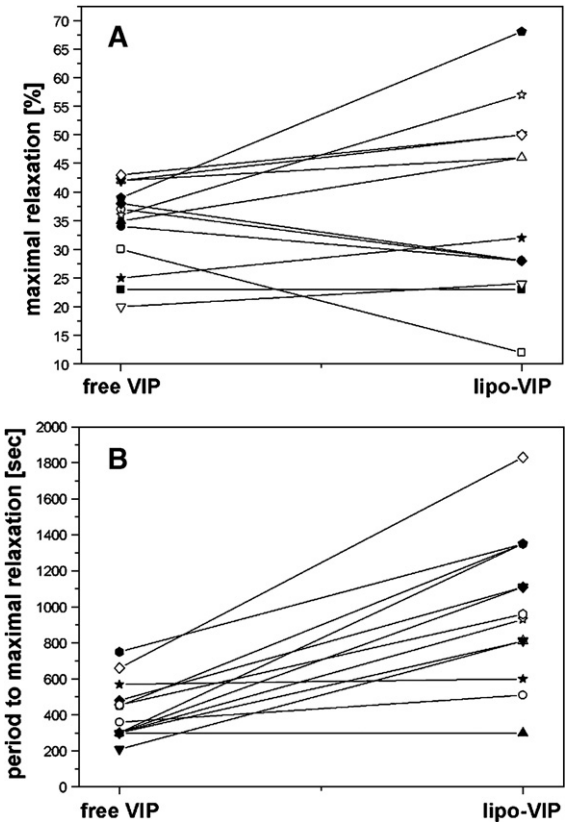


Fig. 5. Vasorelaxation efficiency and relaxation kinetics. Panel A shows the values of the maximal relaxation in % of 100% precontraction with phenylephrine obtained for the pairwise comparison of free VIP with liposomal-associated VIP ($n$=13 pairs). Panel B demonstrates the time period in seconds between administration of VIP and attainment of maximal relaxation for the pairwise comparison of free VIP with liposomal-associated VIP shown in panel A. Each pair is plotted with a specific symbol connected by a straight line.

kinetics for free VIP and liposomal-associated VIP were studied in an *ex vivo* arterial model system performing a pairwise comparison using the same artery. This strategy was chosen to eliminate variations between different arterial preparations. The maximal relaxation observed for free- and liposomal-VIP (34.1±2.1% and 37.8±4.5%, respectively; $n=13$ pairs ) was shown not to be significantly different ($p>0.1$). In contrast, the kinetics, i.e. the time between VIP administration and attaining of the maximal relaxation was significantly ($p<0.001$) delayed for liposomal-associated VIP ( t=1002±115 s) compared to free VIP ( t=418±45 s; $n=13$ pairs). The single values for the relaxation efficiency and kinetics used for the pairwise comparison are shown in Fig. 5A and B, respectively. As control, empty liposomes showed no relaxation activity.

## 4. Discussion

Polymer-grafted unilamellar liposomes were made by the thin-film rehydration method using a ternary mixture of phospholipid species. The lipid mixture was composed of a zwitterionic phosphatidylcholine (POPC) as lipid matrix, a PEGylated lipid (DSPE-PEG2000) to obtain sterical stabilization, and an anionic lysolipid (lyso-PG). Amongst a number of stealth liposomal formulations suggested for drug delivery purposes in the literature (for a comprehensive review see [13]), our formulation is exceptional mainly due to the addition of the negatively charged lysolipid. We decided to use lyso-PG for several reasons. First, the acidic headgroups confer an enhanced negative surface charge to the particle that causes electrostatic repulsion of bilayers. This special feature favors the formation of unilamellar rather than multilamellar vesicles, preferentially formed by phosphatidylcholine. Second, the negative charge of phosphatidylglycerols causes electrostatic attraction of cationic peptides and, in our special case, facilitates efficient peptide loading through peptide–membrane interaction. Third, lysolipids – due to the mono-acyl chain – adopt an inverted-cone shape. Thus, lysolipids have a higher cross-section of the headgroups compared to the fatty acid chain region and maintain a spherical bilayer arrangement by conferring a positive membrane curvature. Hence, a film of this lipid mixture self-assembles upon hydration to unilamellar liposomes with about 95% of the liposomes in a size range up to 200 nm. This particle size distribution would allow for a direct transport of the liposomes to the lower alveolar regions [21,34] without further manipulations of the liposomes. Consequently, treatment by size extrusion is not necessary, although a small subpopulation of particles with sizes up to 550 nm is present in the unextruded preparation. The latter contribution might well be caused by the presence of some rod-like particles, as the algorithm used for the calculation of average size distribution does not distinguish between spherical or rod-like particles.

It is already known that with increasing concentrations of PEG-lipids a transition from spherical vesicles to disks and finally to micellar phases occurs [17,31]. For example, worm-like micelles were reported by Edwards et al. [35] for a binary system consisting of PEG-lipids and egg phosphatidylcholine at molar concentrations above 15 mol% PEG-lipids. At higher PEG-lipid concentrations a final conversion from rod-like micellar structures to spherical micelles takes place [36]. However, for the liposomal formulation reported in this study, the PEG2000-lipid concentration was limited to 5 mol%, a concentration at which DSPE-PEG2000 lipids are already in the so-called brush regime, in which neighboring PEG coils interact laterally, but the phospholipids still form a closed bilayer structure [29]. Indeed, by TEM measurements we could confirm that the liposomes are essentially spheroidal and hollow, although a small fraction of elongated tubular particles was seen in the images. In support, SAXS data showed an uncorrelated bilayer structure without any indication for a non-lamellar phase behavior or for a regular alignment of multilayers.

VIP was associated to the liposomes at a molar ratio of ~0.004 mole VIP / mole phospholipid. For a spherical single bilayer nanoparticle with an average diameter of about 90 nm, which has an outer hydrophilic PEG2000 surface layer in the brush regime with a thickness of about 4.5 nm [29] and a phospholipid bilayer thickness of 4.2 nm, we can estimate the number of lipid molecules that form one vesicle. Assuming an average cross-sectional membrane surface area of 0.65 $nm^2$ for lipids in the fluid phase [37], we have calculated a total number of approximately 60000 lipid molecules for one vesicle, equivalent to about 200 VIP molecules/liposome. However, this value should not be considered as an upper limiting rate, but corresponds to the loading conditions investigated in this study. Importantly, the peptide concentration used here is in a range suited for treatment of lung hypertension, in which the daily administration of 200 μg free VIP via inhalation is required [6]. This value would correspond to a medication of about 400 μl of our formulation per day, however, the therapeutic dose of VIP might well be reduced due to protective effects of the liposomes.

In our system we have performed passive peptide loading, which means, that the formation of liposomes takes place in the presence of the peptide. In this way, we have achieved a quantitative loading of VIP, which could not be separated from the liposomes by column chromatography. However, the question arises whether VIP is encapsulated in the aqueous interior of the vesicle or is associated with the lipid membrane. As it is known that VIP interacts with phospholipids [38–40] it might well align along both the inner and outer leaflet of the bilayer. Such an interaction would be mediated primarily by electrostatic attractions between the polar amino acid residues and the negatively charged phospholipid headgroups of phosphatidylglycerol or/and the negative charge of the phosphate group of PEG-lipids. Additionally, VIP might penetrate the bilayer, stabilized in part by the hydrophobic effect.

To address this issue we have performed a fluorescence study to investigate membrane association properties of VIP. For these experiments we have used single Trp-modified VIP species with the Trp residue being located at different positions along the amino acid sequence. These data indicate that the N-terminal domain of VIP sticks in the membrane and becomes located in a non-polar environment while the central α-helical part and the C-terminal random coiled region are still shielded but not that strong. The protective effect of a polymer coat was

already recognized in a lower susceptibility to enzymatic inactivation in plasma or by trypsin in vitro [41,42]. By analogy, a similar behavior is expected for endopeptidase-modulated degradation of liposomal-VIP in the airways [8,9]. Thus, apart from inducing unilamellarity, the rationale for the incorporation of PEGylated lipids in our formulation was to protect the surface-associated peptide from degradation, rather than to prolong the life-time of the liposome itself. Although, one could speculate that the PEG-coat might be advantageous to reduce liposomal uptake by alveolar macrophages and to diminish phagocytosis.

Besides, we suppose a dual distribution of VIP within the inner and outer leaflet of the liposomes with internally entrapped VIP being completely protected against enzymatic degradation. In this case, surface-associated VIP would be recognized by its receptor first. Entrapped VIP would be released and bound later on upon liposomal degradation. This mechanism could be advantageous for medical applications as a retarded relaxation effect for VIP could be achieved. Indeed, our data from *ex vivo* experiments on active lung arteries displayed a retarded dilatation effect for liposomal-VIP as compared to free VIP.

Despite the association of VIP with the lipophilic environment of the liposomes, we could not detect a significant effect of VIP on the bilayer arrangement. At least at the given lipid to peptide molar ratio neither the bilayer thickness nor the mobility of the phospholipid acyl chains were affected by VIP. One possible explanation could be that the phospholipid acyl chains are not very tightly packed due to the presence of lysolipids. This is supported by the relatively low value determined for the order parameter, which might also reflect some lateral separation of lipid components. In view of the 250-fold excess of lipid molecules the insertion of VIP, which is probably restricted to the interfacial headgroup region, has no impact on the local order parameter of the acyl chains. Likewise, some gap caused by peptide penetration has no appreciable effect on bilayer thickness and some local minor pertubations caused by peptide penetration might be smoothed by global averaging of data.

Our CD data showed that VIP exhibits a conformational change from an unordered random coil structure in aqueous solution to α-helical in liposomes. Such a conformational conversion of VIP was already reported by other groups [42,43] and seems to be mediated by negative charges. Thus, electrostatic attraction of the positively charged peptide by negatively charged phospholipid headgroups is supposed to be the driving force for helix formation subsequently stabilized by the hydrophobic effect through membrane anchoring.

Molecular modeling has shown that VIP could form an α-helix, spanning the central amino acid residues from $Val^5$ to $Asn^{24}$ with random coiled N- and C-terminus [44]. These data were confirmed by a recent NMR study that describes $Thr^7$–$Asn^{24}$ as central helical element [22]. Consistently, the secondary structure prediction performed in this study reveals an α-helical region starting from $Tyr^{10}$, with high prediction confidence. A helical wheel projection of this region clearly shows an asymmetrical distribution of polar and apolar residues of VIP. Thereby, hydrophobic and hydrophilic residues segregate on opposing sides of the helix to form an amphipathic helix, which is a common feature of many membrane-active peptides [45–47]. Notably, in our cylindrical projection along the helix axis most of the positively charged lysine and arginine residues, which are supposed to interact with the acidic phospholipids, are located at the same side as the hydrophobic residues.

By receptor binding studies it was outlined that the important amino acids for receptor binding are distributed along the peptide chain from position 1 to 26 [44]. Similarly, docking experiments of VIP to VPAC1 show the direct involvement of the amino acid sequence 6 to 28 converted in an α-helical conformation in receptor binding. The N-terminal segment is largely disorded as shown by NMR [22] and forms a bent conformation as found by computational methods on amino acids 1 to 11 using simulated annealing [48]. This N-terminal region was suggested to interact independently with a second receptor domain [22]. In our study we found that this segment is trapped in the bilayer, but might become released upon receptor binding. In any case, the helical conformation relevant for receptor interaction is induced and stabilized by lipid interaction, whereas the helical part of VIP is most probably located parallel to the membrane. These α-helical stabilizing properties of negatively charged vesicles could explain the higher receptor activity reported for liposomal-VIP [38,49] as well as the pronounced vasodilatory effect exerted in peripheral microcirculation [40,50]. These data are also supported by our results on the relaxation behavior of active lung arteries in the presence of VIP. These experiments clearly demonstrate that liposomal-associated VIP is set free in the course of receptor binding to trigger the observed vasodilation with comparable efficiency as free VIP. However, the time point of maximal relaxation is significantly delayed by liposomes indicating a retarded effect on vasorelaxation. Nevertheless, it has to be mentioned that the lung artery model system cannot reflect directly the *in vivo* situation after aerosolic application.

In summary, for our approach we have prepared liposomes which form stable unilamellar bilayer spheres in a size range to be used for aerosolic delivery to the lung without further manipulations [21,34].

The polymer-grafted liposomes were able to accommodate reasonable amounts of active VIP to be considered for medical treatment of PPH patients [6].

In addition, the interaction mechanisms of VIP with lipid membranes were thoroughly investigated and the structural data might be helpful for studies on receptor binding and provide useful information for further developments of therapeutical applications of this neuropeptide.

## Acknowledgements

The Austrian Nano-Initiative co-financed this work as part of the Nano-Health project (no. 0200), the sub-projects NANO-LIPO, NANO-BREATH, NANO-MRI being financed by the Austrian FWF (Fonds zur Förderung der Wissenschaftlichen

Forschung) Project no. N202, N206, N201, respectively and NANO-VIP by the FFF (Project no.253-NAN).

We are grateful to Bernadette Zanner, Dorina Clay and Silvia Fill for technical assistance.

## References

[1] I.M. Keith, The role of endogenous lung neuropeptides in regulation of the pulmonary circulation, Physiol. Res. 49 (2000) 519–537.
[2] N.A. Hasaneen, H.D. Foda, S.I. Said, Nitric oxide and vasoactive intestinal peptide as co-transmitters of airway smooth-muscle relaxation: analysis in neuronal nitric oxide synthase knockout mice, Chest 124 (2003) 1067–1072.
[3] M. Delgado, D. Pozo, D. Ganea, The significance of vasoactive intestinal peptide in immunomodulation, Pharmacol. Rev. 56 (2004) 249–290.
[4] I. Gozes, S. Furman, VIP and drug design, Curr. Pharm. Des. 9 (2003) 483–494.
[5] D.A. Groneberg, K.F. Rabe, A. Fischer, Novel concepts of neuropeptide-based drug therapy: vasoactive intestinal polypeptide and its receptors, Eur. J. Pharmacol. 533 (2006) 182–194.
[6] V. Petkov, W. Mosgoeller, R. Ziesche, M. Raderer, L. Stiebellehner, K. Vonbank, G.C. Funk, G. Hamilton, C. Novotny, B. Burian, L.H. Block, Vasoactive intestinal peptide as a new drug for treatment of primary pulmonary hypertension, J. Clin. Invest. 111 (2003) 1339–1346.
[7] E.K. Tam, G.M. Franconi, J.A. Nadel, G.H. Caughey, Protease inhibitors potentiate smooth muscle relaxation induced by vasoactive intestinal peptide in isolated human bronchi, Am. J. Respir. Cell Mol. Biol. 2 (1990) 449–452.
[8] M. Hachisu, T. Hiranuma, S. Tani, T. Iizuka, Enzymatic degradation of helodermin and vasoactive intestinal polypeptide, J. Pharmacobiodyn. 14 (1991) 126–131.
[9] C.M. Lilly, J.M. Drazen, S.A. Shore, Peptidase modulation of airway effects of neuropeptides, Proc. Soc. Exp. Biol. Med. 203 (1993) 388–404.
[10] D.D. Lasic, Novel applications of liposomes, Trends Biotech. 16 (1998) 307–321.
[11] T. Lian, R.J. Ho, Trends and developments in liposome drug delivery systems, J. Pharm. Sci. 90 (2001) 667–680.
[12] T.M. Allen, P.R. Cullis, Drug delivery systems: entering the mainstream, Science 303 (2004) 1818–1822.
[13] V.P. Torchilin, Recent advances with liposomes as pharmaceutical carriers, Nat. Rev., Drug Discov. 4 (2005) 145–160.
[14] G. Blume, G. Cevc, Liposomes for the sustained drug release in vivo, Biochim. Biophys. Acta 1029 (1990) 91–97.
[15] D. Papahadjopoulos, T.M. Allen, A. Gabizon, E. Mayhew, K. Matthay, S.K. Huang, K.D. Lee, M.C. Woodle, D.D. Lasic, C. Redemann, Sterically stabilized liposomes: improvements in pharmacokinetics and antitumor therapeutic efficacy, Proc. Natl. Acad. Sci. U. S. A. 88 (1991) 11460–11464.
[16] M.C. Woodle, L.R. Collins, E. Sponsler, N. Kossovsky, D. Papahadjopoulos, F.J. Martin, Sterically stabilized liposomes. Reduction in electrophoretic mobility but not electrostatic surface potential, Biophys. J. 61 (1992) 902–910.
[17] M.C. Woodle, M.S. Newman, J.A. Cohen, Sterically stabilized liposomes: physical and biological properties, J. Drug Target 2 (1994) 397–403.
[18] Y. Barenholz, Liposome application: problems and prospects, Curr. Opin. Colloid Interface Sci. 6 (2001) 66–77.
[19] T.M. Allen, C. Hansen, Pharmacokinetics of stealth versus conventional liposomes: effect of dose, Biochim. Biophys. Acta 1068 (1991) 133–141.
[20] T.M. Allen, Liposomal drug formulations. Rationale for development and what we can expect for the future, Drugs 56 (1998) 747–756.
[21] N.R. Labiris, M.B. Dolovich, Pulmonary drug delivery. Part II: the role of inhalant delivery devices and drug formulations in therapeutic effectiveness of aerosolized medications, Br. J. Clin. Pharmacol. 56 (2003) 600–612.
[22] Y.V. Tan, A. Couvineau, S. Murail, E. Ceraudo, J.M. Neumann, J.J. Lacapere, M. Laburthe, Peptide agonist docking in the N-terminal ectodomain of a Class II G Protein-coupled receptor, the VPAC1 receptor: PHOTOAFFINITY, NMR, and MOLECULAR MODELING, J. Biol. Chem. 281 (2006) 12792–12798.
[23] G.R. Bartlett, J. Biol. Chem 234 (1959) 466–468.
[24] A. Bergmann, G. Fritz, O. Glatter, Solving the generalized indirect Fourier transformation (GIFT) by Boltzmann simplex simulated annealing (BSSA), J. Appl. Cryst. 33 (2000) 1212–1216.
[25] A. Lobley, L. Whitmore, B.A. Wallace, DICHROWEB: an interactive website for the analysis of protein secondary structure from circular dichroism spectra, Bioinformatics 18 (2002) 211–212.
[26] L. Whitmore, B.A. Wallace, DICHROWEB, an online server for protein secondary structure analyses from circular dichroism spectroscopic data, Nucleic Acids Res. 32 (2004) W668–W673.
[27] K. Bryson, L.J. McGuffin, R.L. Marsden, J.J. Ward, J.S. Sodhi, D.T. Jones, Protein structure prediction servers at University College London, Nucleic Acids Res. 33 (2005) W36–W38.
[28] L.J. McGuffin, K. Bryson, D.T. Jones, The PSIPRED protein structure prediction server, Bioinformatics 16 (2000) 404–405.
[29] O. Garbuzenko, Y. Barenholz, A. Priev, Effect of grafted PEG on liposome size and on compressibility and packing of lipid bilayer, Chem. Phys. Lipids 135 (2005) 117–129.
[30] A.K. Kenworthy, K. Hristova, D. Needham, T.J. McIntosh, Range and magnitude of the steric pressure between bilayers containing phospholipids with covalently attached poly(ethylene glycol), Biophys. J. 68 (1995) 1921–1936.
[31] D. Marsh, R. Bartucci, L. Sportelli, Lipid membranes with grafted polymers: physicochemical aspects, Biochim. Biophys. Acta 1615 (2003) 33–59.
[32] S.Y. Venyaminov, J.T. Yang, Determination of Protein Secondary Structure, in: G.D. Fasman (Ed.), Circular Dichroism and the Conformational Analysis of Biomolecules, Plenum Press, New York, London, 1 pp. 69–108.
[33] D.T. Jones, Protein secondary structure prediction based on position-specific scoring matrices, J. Mol. Biol. 292 (1999) 195–202.
[34] R. Abu-Dahab, U.F. Schäfer, C.M. Lehr, Lectin-functionalized liposomes for pulmonary drug delivery: effect of nebulization on stability and bioadhesion, Eur. J. Pharm. Sci. 14 (2001) 37–46.
[35] K. Edwards, M. Johnson, G. Karlsson, M. Silvander, Effect of polyethyleneglycol-phospholipids on aggregate structure in preparations of small unilamellar liposomes, Biophys. J. 73 (1997) 258–266.
[36] L. Arleth, B. Ashok, H. Onyuksel, P. Thiyagarajan, J. Jacob, R.P. Hjelm, Detailed structure of hairy mixed micelles formed by phosphatidylcholine and PEGylated phospholipids in aqueous media, Langmuir 21 (2005) 3279–3290.
[37] D. Marsh, Handbook of Lipid Bilayers, in: D. Marsh (Ed.), Handbook of Lipid Bilayers, CRC Press Inc., Boca Raton, FL, 1990, pp. 387–393.
[38] Y. Noda, J. Rodriguez-Sierra, J. Liu, D. Landers, A. Mori, S. Paul, Partitioning of vasoactive intestinal polypeptide into lipid bilayers, Biochim. Biophys. Acta 1191 (1994) 324–330.
[39] H. Ikezaki, S. Paul, H. Alkan-Onyuksel, M. Patel, X.P. Gao, I. Rubinstein, Vasodilation elicited by liposomal VIP is unimpeded by anti-VIP antibody in hamster cheek pouch, Am. J. Physiol. 275 (1998) R56–R62.
[40] H. Onyuksel, B. Ashok, S. Dagar, V. Sethi, I. Rubinstein, Interactions of VIP with rigid phospholipid bilayers: implications for vasoreactivity, Peptides 24 (2003) 281–286.
[41] X.P. Gao, Y. Noda, I. Rubinstein, S. Paul, Vasoactive intestinal peptide encapsulated in liposomes: effects on systemic arterial blood pressure, Life Sci. 54 (1994) L247–L252.
[42] G. Gololobov, Y. Noda, S. Sherman, I. Rubinstein, J. Baranowska-Kortylewicz, S. Paul, Stabilization of vasoactive intestinal peptide by lipids, J. Pharmacol. Exp. Ther. 285 (1998) 753–758.
[43] I. Rubinstein, M. Patel, H. Ikezaki, S. Dagar, H. Onyuksel, Conformation and vasoreactivity of VIP in phospholipids: effects of calmodulin, Peptides 20 (1999) 1497–1501.
[44] P. Nicole, L. Lins, C. Rouyer-Fessard, C. Drouot, P. Fulcrand, A. Thomas, A. Couvineau, J. Martinez, R. Brasseur, M. Laburthe, Identification of key residues for interaction of vasoactive intestinal peptide with human VPAC1 and VPAC2 receptors and development of a highly selective

VPAC1 receptor agonist. Alanine scanning and molecular modeling of the peptide, J. Biol. Chem. 275 (2000) 24003–24012.
[45] J.A. Gazzara, M.C. Phillips, S. Lundkatz, M.N. Palgunachari, J.P. Segrest, G.M. Anantharamaiah, J.W. Snow, Interaction of class A amphipathic helical peptides with phospholipid unilamellar vesicles, J. Lipid Res. 38 (1997) 2134–2146.
[46] R.M. Epand, R.F. Epand, R.C. Orlowski, R.J. Schlueter, L.T. Boni, S.W. Hui, Amphipathic helix and its relationship to the interaction of calcitonin with phospholipids, Biochemistry 22 (1983) 5074–5084.
[47] R.M. Epand, Y. Shai, J.P. Segrest, G.M. Anantharamaiah, Mechanisms for the modulation of membrane bilayer properties by amphipathic helical peptides, Biopolymers 37 (1995) 319–338.
[48] M. Filizola, M. Carteni-Farina, J.J. Perez, Conformational study of vasoactive intestinal peptide by computational methods, J. Pept. Res. 50 (1997) 55–64.
[49] M. Huang, O.P. Rorstad, VIP receptors in mesenteric and coronary arteries: a radioligand binding study, Peptides 8 (1987) 477–485.
[50] F. Sejourne, H. Suzuki, H. Alkan-Onyuksel, X.P. Gao, H. Ikezaki, I. Rubinstein, Mechanisms of vasodilation elicited by VIP in sterically stabilized liposomes in vivo, Am. J. Physiol. 273 (1997) R287–R292.